

1  
2  
3  
4  
5  
6  
7  
8  
9  
10  
11  
12  
13  
14  
15  
16  
17  
18  
19

Climatic control of intra-annual wood density fluctuations of  
*Pinus pinaster* in NW Spain

Vicente Rozas <sup>1,\*</sup>, Ignacio García-González <sup>2</sup>, Rafael Zas <sup>1</sup>

<sup>1</sup> Misión Biológica de Galicia, Consejo Superior de Investigaciones Científicas, Apdo.  
28, E-36080 Pontevedra, Spain

<sup>2</sup> Departamento de Botánica, Escola Politécnica Superior, Campus de Lugo,  
Universidade de Santiago de Compostela, E-27002 Lugo, Spain

\* Corresponding author: E-mail [vrozas@mbg.cesga.es](mailto:vrozas@mbg.cesga.es) , Telephone +34 986 854800,  
Fax +34 986 841362

20

21 **Abstract** Tree rings of *Pinus pinaster* often contain intra-annual density fluctuations  
22 (IADFs), which have been attributed to the succession of dry and rainy periods typical  
23 of Mediterranean climate, but their formation has not been studied yet under Atlantic  
24 climate. We analyzed the occurrence and climatic significance of replicated IADFs in  
25 ten monospecific stands in NW Spain. The frequency of IADFs was higher than  
26 previously reported for this species under Mediterranean conditions and consistently  
27 decreased with increasing elevation. The formation of bands of latewood-like tracheids  
28 within the earlywood was favored by dry previous August, cold previous winter and dry  
29 April. Bands of earlywood-like tracheids within the early latewood were also favored by  
30 low winter temperatures. However, their occurrence was geographically heterogeneous,  
31 with two groups of stands being defined by their distances to the shoreline. In coastal  
32 stands, cold May-August triggered IADFs formation, while in inland stands their  
33 formation was favored by dry May-July. Regional winter temperatures and April water  
34 balance were strongly related to the East Atlantic (EA) pattern, which greatly  
35 conditioned the occurrence of IADFs in the earlywood and the early latewood. By  
36 contrast, the presence of bands of earlywood-like tracheids in the late latewood was  
37 independent of the EA pattern, being strongly related to warm conditions in spring and  
38 especially to a wet October. The link between regional climate and the EA pattern  
39 strongly controlled the physiological processes that determine intra-annual growth  
40 dynamics and short-term cell enlargement of *P. pinaster* in NW Spain.

41

42 **Keywords** Dendrochronology, false tree-rings, *Pinus pinaster*, Atlantic climate, water  
43 balance, East Atlantic pattern

44

## 45 **Introduction**

46 The integration of the effects of several environmental factors operating at multiple time  
47 scales on tree-ring growth make difficult to understand the underlying mechanisms  
48 responsible for triggering intra-annual cambial activity and growth dynamics (Fritts  
49 2001). In fact, cambial activity in conifers may vary at a shorter time scale within the  
50 growing season, leading to the formation of intra-annual bands of tracheids with  
51 distinctive appearance, differing from those typical of the early- or latewood parts of the  
52 ring (Vaganov et al. 2009). Like the most widely used ring-width records, small  
53 variations in wood density within a tree ring are morphologically preserved in the wood  
54 structure and can be easily differentiated and analyzed any time.

55 The intra-annual density fluctuations (IADFs) in conifers are areas of the tree ring  
56 where wood density changes as a response to a particular combination of environmental  
57 conditions that modify the rates of cambial activity (De Micco et al. 2007). The term  
58 IADF includes the so-called false rings, intra-annual bands, light latewood rings and  
59 double or multiple rings, which can be anatomically characterized by latewood-like  
60 tracheids within the earlywood, or earlywood-like tracheids within the latewood  
61 (Wimmer et al. 2000; Girardin et al. 2001; Rigling et al. 2001). The visual  
62 characterization of IADFs is given by changes in the wall/lumen ratio of the tracheids,  
63 which corresponds with intra-ring variations in the  $^{13}\text{C}/^{12}\text{C}$  isotopic composition of  
64 cellulose, suggesting that IADFs are associated to plastic responses to changes in  
65 physiological stress (Park et al. 2006; De Micco et al. 2007).

66 Several external disturbance events such as insect outbreaks, and different climatic  
67 triggers such as droughts, flooding, snowfall, or frosts have been identified as causes of  
68 IADF formation (Rigling et al. 2002; Hoffer and Tardif 2009; Edmondson 2010). In

69 addition, individual features such as canopy position, growth rate and tree age can also  
70 influence their formation (Copenheaver et al. 2006; Bogino and Bravo 2009; Vieira et  
71 al. 2009). Usually, the presence of IADFs in the earlywood is related to dry springs  
72 followed by moist conditions, while moist summers can cause IADFs in the latewood  
73 (Wimmer et al. 2000; Bouriaud et al. 2005). A wide variety of woody species under  
74 Mediterranean climate characterized by summer drought and a high inter-annual  
75 variability in precipitation and temperature commonly form IADFs (Cherubini et al.  
76 2003). Among these species, IADFs in the Mediterranean pines *P. halepensis*, *P.*  
77 *pinaster* and *P. pinea* have been attributed to an irregular rainfall regime during the  
78 growing season (Campelo et al. 2006; De Luis et al. 2007; De Micco et al. 2007;  
79 Bogino and Bravo 2009).

80 *Pinus pinaster* is a forest species of the western Mediterranean basin, inhabiting a  
81 wide range of environmental and physiographic conditions. Its main populations are  
82 located in the Iberian Peninsula, growing in both natural and planted woodlands under  
83 climatic conditions ranging from the extremely dry and warm summers of the  
84 Mediterranean areas in central and southern Spain to the mild and humid climate of the  
85 Atlantic coast at its western range boundary in the Iberian Peninsula (Alía et al. 1997).  
86 Despite the great productive and conservational importance of *P. pinaster* under  
87 Atlantic conditions, its intra-annual growth dynamics and sensitivity to limiting climatic  
88 factors have not been studied in this region yet. Under Mediterranean climate, *P.*  
89 *pinaster* presents IADFs in both the early- and latewood due to the succession of dry  
90 and rainy periods during the growing season (Bogino and Bravo 2009; Vieira et al.  
91 2009). The pronounced genetic and physiological differences between the Atlantic and  
92 Mediterranean populations (Bucci et al. 2007; Correia et al. 2008), and the contrasting  
93 climatic regimes of both regions, suggest that other environmental factors different from

94 the alternation between dry and wet periods may be critical for the intra-annual growth  
95 dynamics of *P. pinaster* under Atlantic climate.

96 Regional climate in Spain is controlled by large-scale circulation patterns, such as  
97 the North Atlantic Oscillation and El Niño-Southern Oscillation, which significantly  
98 influence rainfall regimes (Rodó et al. 1997; Trigo et al. 2004). Therefore, large-scale  
99 climatic patterns may also influence intra-annual growth of *P. pinaster* through  
100 determining the variability of regional climate conditions in NW Spain. This study is  
101 aimed at (a) characterizing the occurrence patterns of intra-annual wood density  
102 fluctuations in *Pinus pinaster* over a tree-ring network at its northwestern range  
103 boundary in NW Spain, and (b) identifying the regional and large-scale climatic factors  
104 that drive the formation of different IADF types under Atlantic climate.

105

## 106 **Materials and methods**

### 107 Study area

108 The study area comprises the region of Galicia, NW Spain, where *P. pinaster* grows at  
109 its northwestern range boundary and covers over 47% of the forested area in pure or  
110 mixed stands, being one of the most important commercial woods. Since the past  
111 century, this species has been extensively planted in Galicia (Fig. 1a), and the resulting  
112 even-aged stands are typically managed through short rotations of 40-50 years.  
113 Regional climate is temperate and humid, with a mean annual temperature of 12.7 °C  
114 for the period 1967–2005, ranging between 10.1 and 14.5 °C. The mean annual  
115 precipitation is 1,300 mm, ranging from 870 in the southern inland area to 1,800 mm  
116 near the coast under more oceanic influence.

117

### 118 Climate data

119 We used monthly gridded data from the datasets of the Climate Research Unit,  
120 University of East Anglia (CRU TS 3,  $0.5^\circ \times 0.5^\circ$ ), taken from the Web site of the Royal  
121 Netherlands Meteorological Institute (<http://climexp.knmi.nl/>), for mean temperature  
122 (T) and total precipitation (P) for the period 1967–2006. Since maximum temperature is  
123 coupled to a minimum of rainfall during summer time, precipitation data were just used  
124 to calculate water balance (WB) as  $WB = P - PET$ , where PET is the potential  
125 evapotranspiration estimated as a function of monthly mean temperatures and  
126 geographical latitude (Thornthwaite 1948). Mean monthly WB ranged between  $-73$  mm  
127 in July and  $145$  mm in December-January, showing a tendency to water deficit from  
128 June to August. To characterize the climatic determinants of IADFs formation in *P.*  
129 *pinaster* at a regional scale, mean values from the  $0.5^\circ \times 0.5^\circ$  grid boxes comprised  
130 within the region ( $7.0-9.5^\circ$  W,  $42.0-44.0^\circ$  N) were calculated.

131 Monthly indices of a series of teleconnective patterns (North Atlantic Oscillation,  
132 East Atlantic pattern, East Atlantic/West Russia pattern, Scandinavia pattern,  
133 Tropical/Northern Hemisphere pattern, Polar/Eurasia pattern) were obtained from the  
134 Web site of the NOAA/National Weather Service, Climate Prediction Center, Maryland,  
135 USA ([ftp://ftp.cpc.ncep.noaa.gov/wd52dg/data/indices/tele\\_index.nh](ftp://ftp.cpc.ncep.noaa.gov/wd52dg/data/indices/tele_index.nh)). Among them,  
136 only the East Atlantic (EA) pattern showed significant relationships with IADFs records  
137 of *P. pinaster*. EA pattern is a prominent mode of low-frequency variability structurally  
138 similar to the NAO, which consists of a north-south dipole of anomaly centers spanning  
139 the North Atlantic from east to west, whose positive phase is associated with above-  
140 average surface temperatures in Europe (Barnston and Livezey 1987).

141 Monthly climatic variables were seasonalized to values for winter (December-  
142 February), spring (March-May), summer (June-August) and autumn (September-  
143 November). The considered window for exploring the relations between climate and

144 tree growth were from previous June (Jun(-1)) to current November (Nov) for monthly  
145 values, while for seasonal values they spanned from previous summer (Sum(-1)) to  
146 current autumn (Aut). Additionally, annual values were calculated by averaging  
147 monthly values from previous October (Oct (-1)) to current September (Sep).

148

149 Sampling, tree-ring dating and tree age estimation

150 We sampled 10 monospecific stands located both at the coastal and inland areas along  
151 the full elevation range of *P. pinaster* in Galicia, from sea level to 855 m (Fig. 1b, Table  
152 1). We measured DBH (bole diameter at 1.30 m), and took at least two increment cores  
153 per tree from 15 to 24 dominant trees per stand. The cores were air-dried, glued onto  
154 wooden mounts, and polished with successively finer grades of sandpaper, until the  
155 xylem cellular structure was visible in the transverse plane. The tree-ring series were  
156 absolutely dated by assigning calendar years to the rings following standard procedures  
157 (Fritts 2001). Total ring widths were measured under magnification to the nearest 0.001  
158 mm with a sliding-stage micrometer (Velmex Inc., Bloomfield NY, USA) interfaced  
159 with a computer. The software COFECHA (Grissino-Mayer 2001) was used to  
160 quantitatively check for crossdating errors in the ring width series. All series with  
161 potential dating errors or weakly correlated with the master site chronology were  
162 corrected when possible or discarded.

163 In cores showing the pith, tree age at coring height was determined by the number  
164 of crossdated rings. In partial cores showing the arcs of the inner rings, the pith was  
165 located using a graphical method based on the convergence of xylem rays at the pith  
166 (Rozas 2003), and the number of missing rings toward the pith was estimated by  
167 extrapolating the mean growth rates from the innermost five rings in the cores. Tree age

168 was estimated based on the oldest core per tree. No corrections for the number of  
169 missing rings due to coring height were performed.

170

171 Intra-annual wood density fluctuations

172 The adequately dated cores were visually examined under magnification for  
173 identification of IADFs, which were distinguished from actual tree rings due to their  
174 non-sharp transitions in opposite to the marked boundaries between annual rings  
175 (Wimmer et al. 2000; Park et al. 2006). Based on previous definitions for *P. pinaster*,  
176 IADFs were classified into three types according to their appearance and intra-ring  
177 position (Vieira et al. 2009). IADFs type E were bands of latewood-like tracheids within  
178 the earlywood (Fig. 2a). By contrast, IADFs types L and L+ were bands of earlywood-  
179 like tracheids within the latewood (Fig. 2b), and near the transition between the  
180 latewood and the earlywood of the following ring (Fig. 2c), respectively.

181 An IADF in a given ring was considered when present in at least one core per tree,  
182 and was tabulated. The percent frequencies of cores and rings per stand showing IADFs  
183 of types E, L, and L+ were computed as descriptive statistics of the IADF distributions.  
184 The relative frequency of IADFs was calculated as  $F = n_x/N$ , where  $n_x$  is the number of  
185 trees showing IADFs in the year  $x$ , and  $N$  is the number of trees in that year. Moreover,  
186 the variance bias induced by the varying number of tree rings per year was corrected by  
187 calculating the stabilized IADF frequency as  $F_{stab} = F \times N^{0.5}$  (Rigling et al. 2001).  $F_{stab}$   
188 series were calculated separately for the types E, L and L+ at each stand. In order to  
189 estimate the dependence of IADFs frequency on ring age and ring width, Spearman's  
190 correlations between ring age, mean ring width, and  $F_{stab}$  of each IADF type, were  
191 calculated.



192 We tested if the occurrence of IADFs in *P. pinaster* was independent from both  
193 inter-site distances and differences between site elevations using the standardized  
194 Mantel statistic ( $R_M$ ). The Mantel test compares two similarity or distance matrices  
195 computed for the same objects, and behaves like a correlation coefficient, being  
196 bounded between  $-1$  and  $1$  (Legendre and Legendre 1998). To calculate  $R_M$  we used the  
197 matrices of similarity between  $F_{\text{stab}}$  chronologies and descriptive statistics of the IADF  
198 distributions for the period 1967-2005, compared to the matrices of geographical  
199 distances and elevation differences among stands. We used Spearman's correlation as a  
200 measure of similarity between  $F_{\text{stab}}$  chronologies, and  $1 - D_{\text{norm}}$  as similarity between  
201 descriptive statistics, being  $D_{\text{norm}}$  the normalized difference ranging between 0 and 1  
202 (Legendre and Legendre 1998). Since we compared similitude matrices with distance  
203 matrices, positive and negative  $R_M$  values would indicate more and less similar patterns,  
204 respectively, at increasing distances or elevation differences. The statistical significance  
205 of  $R_M$  was tested by means of 9,999 random permutations of one of the distance  
206 matrices, to obtain the expected distribution of the statistic under the null hypothesis of  
207 independence.  $R_M$  was calculated with the Mantel function from the PopTools v3.1.0  
208 add-in for Microsoft Excel (<http://poptools.org/>).

209

#### 210 Relationships between IADFs and climate variability

211 To analyze the relationships between climate and IADFs frequency at a regional scale,  
212 we excluded from the analyses those years showing IADF frequencies that did not show  
213 any significant replication within a stand. We used the definition given by  
214 Schweingruber et al. (1990) of "pointer year" to refer to a group of trees in which most  
215 of them display an event –in our case a density fluctuation– in the same year. The most  
216 conspicuous IADFs replicated amongst a significant proportion of trees at each stand

217 were considered using a significance test that identifies frequencies higher than a given  
218 background value (Edmondson 2010). This background value represents the  
219 approximate frequency of an entirely random inter-annual occurrence, and was  
220 calculated as the ratio between all IADFs and the total number of dated rings at a given  
221 stand. The frequency  $F$  was considered significant when the value  $F - (F \cdot (1 - F) / N)^{0.5}$   
222 exceeded the random background value (Edmondson 2010). Pointer years showing  
223 significant IADFs were identified separately for the types E, L and L+ in each stand,  
224 and a regional distribution was calculated for each type as the year-by-year sum of  
225 significant events at all stands (Appendix S1).

226 The analyses for relating climate and IADFs frequency were performed along  
227 1967–2005, the common period for all IADFs records. Due to the abundant zero values  
228 in the regional chronology of IADFs type E, we calculated the anomalies of all climatic  
229 variables for pointer years in comparison to the expected means in the remainder years  
230 without IADFs for the period of analysis (Masiokas and Villalba 2004). Monthly,  
231 seasonal and annual climatic variables were normalized, and the deviations of means  
232 from years showing IADFs type E, with respect to years not showing IADFs, were  
233 calculated. Standard deviations above 0.5 or below –0.5 were considered as significant  
234 positive or negative anomalies, respectively. Logistic regression analysis was also used  
235 to identify those independent explanatory variables with a significant effect on the  
236 probability of occurrence of IADFs type E at a regional level. The model was depicted  
237 by  $P = 1 / (1 + e^{a + \sum b_i X_i})$ , where  $P$  is the probability of an IADF occurrence ( $P = 0$  indicates  
238 non-pointer year,  $P = 1$  indicates pointer year),  $a$  is the constant of the model and  $b_i$  are  
239 the coefficients for the independent variables  $X_i$ . Logistic regression was performed by  
240 a forward stepwise procedure and the best adjustment was obtained by maximum  
241 likelihood (Sokal and Rohlf 1995).

242 For IADFs types L and L+, the reduced number of null values allowed the use of  
243 correlation analysis to identify the main climatic variables that determined the regional  
244 IADF chronologies. To account for non-normality of regional IADF pointer-year  
245 chronologies, we calculated Spearman's rank correlations between the regional  
246 chronologies of types L and L+ and the monthly, seasonal and annual climatic variables.  
247 Additionally, to evaluate the diversity of climatic triggers at a local scale, Spearman's  
248 correlations between local  $F_{stab}$  distributions and monthly gridded T and WB were  
249 calculated. Finally, the relationships between regional climate variability and EA pattern  
250 were explored by means of Pearson's correlation. The statistical analyses were  
251 performed with the SPSS 15.0 for Windows package (SPSS Inc., Chicago IL, USA).

252

## 253 **Results**

### 254 Characteristics of trees and IADF distributions

255 The mean DBHs of dominant trees at the sampled stands varied between 29.6–66.7 cm,  
256 and the mean estimated ages between 33–55 years (Table 1). The reduced standard  
257 deviations of tree ages suggested an even-aged origin for the majority of the sampled  
258 stands. Almost 100% of the 498 cores analyzed showed IADFs (Table 2). The  
259 proportion of cores with IADFs type E was quite variable, ranging between 2.2 and  
260 88.2%, while the proportion of cores with IADFs in the latewood was consistently high.  
261 For IADFs type L, the proportions ranged between 58.3–100%, and 87.5–100% for the  
262 type L+. A total of 19,513 tree rings were analyzed, with the proportion of rings with  
263 IADFs varying between 15.9–89.5% depending on the site. The proportion of rings  
264 showing IADFs type E ranged between 0.0–9.0%, while the types L and L+ were  
265 comparatively more abundant, ranging between 3.7–38.8% for type L, and 7.9–66.9%  
266 for type L+.

267

268 Patterns of IADFs occurrence

269 No inter-site common trends in the relationships between the frequency of IADFs and  
270 tree-ring age or ring widths were found. For the IADFs type E, there were no significant  
271 relationships of  $F_{\text{stab}}$  with age and ring width. For types L and L+ some correlations  
272 were statistically significant, both positive and negative, but no general pattern was  
273 observed (Appendices S1, S2).

274 The similitude between  $F_{\text{stab}}$  chronologies was neither related to inter-site  
275 distances nor to the difference among site elevations, as shown by the Mantel test  
276 (Table 3). The only exception was the IADFs type L, which showed a negative  
277 relationship with inter-site distances, suggesting less similar patterns of IADFs  
278 frequency when increasing distance. The statistics for IADFs distribution were  
279 independent of the geographic distance, but were in general significantly and negatively  
280 related to elevation differences. Additionally, negative correlations with elevation were  
281 found for the proportion of cores showing IADFs types E ( $R = -0.71$ ,  $P = 0.021$ ) and L  
282 ( $R = -0.65$ ,  $P = 0.041$ ). The only exception was the proportion of cores showing IADFs  
283 type L+, which did not show a great inter-site variation. These results suggest more  
284 frequent IADFs occurring at lower than at higher sites, irrespective of their geographical  
285 position.

286

287 Climatic significance of IADFs

288 Composite regional distributions of pointer years for significant IADFs were developed  
289 for each IADF type, according to the random background frequencies for pointer year  
290 recognition (Appendix S1). For IADFs type E, the 16 pointer years within the period  
291 1967–2005 showed below-average temperature in December and previous winter,

292 below-average water balance in previous August and April, and below-average EA  
293 indices in previous December and April (Fig. 3a). According to the logistic model, the  
294 independent explanatory variables with a positive effect on the probability of  
295 occurrence of IADFs type E were lower EA indices in April (Wald's test  $\chi^2 = 4.94$ ,  $P =$   
296  $0.026$ , coefficient  $b = -0.009$ ), and reduced water balance in previous August ( $\chi^2 = 4.27$ ,  
297  $P = 0.039$ ,  $b = -0.038$ ).

298 The regional record of pointer years showing IADFs of type L was significantly  
299 correlated with both T and EA variability, but independent from any variation in WB  
300 (Fig. 3b). Pointer years for IADFs type L were negatively correlated with winter and  
301 annual T, and also with EA variation in previous December, previous winter, and its  
302 annual variation. The local distributions of  $F_{stab}$  for IADFs type L were negatively  
303 correlated with T in January-February and May-August at the coastal sites (CAP, COR,  
304 INS, MUR, VIG), but in the period May-August positive correlations with T were  
305 found at inland sites (ALO, BAR, MCU, VER) (Fig. 4a). Moreover,  $F_{stab}$  for IADFs  
306 type L in these inland sites showed also negative correlations with WB in May-July. All  
307 these results suggest that temperature and water availability in the growing season are  
308 site-dependent triggers for IADFs type L formation, exerting contrasting local effects on  
309 intra-annual cambial activity.

310 By contrast, the regional record of pointer years for IADFs type L+ is significantly  
311 correlated with both T and WB variability, but independent from EA pattern (Fig. 3c).  
312 Positive correlations with T in April, August, spring, and the complete year were found.  
313 For WB, positive correlations were found in October and autumn, and negative  
314 correlations in January and the complete year, were found. The local analysis showed  
315 that, in more than 50% of the cases and without any distinction between the coastal and  
316 inland stands, IADFs type L+ responded positively to T in March-May and August, and

317 also positively to WB in October (Fig. 4b). Moreover, high WB in May impacted  
318 negatively on the formation of IADFs type L+.

319 According to the obtained correlations, the main regional climate driver for the  
320 formation IADFs type L was previous winter T, which showed a decreasing number of  
321 pointer years strongly related to the ascending trend of winter temperature (Fig. 5a). For  
322 the type L+, the main climatic driver at a regional scale was autumn WB, with more  
323 frequent IADFs in those years with enough water availability in autumn (Fig. 5b).

324 Several climatic factors revealed as major determinants of IADFs formation in *P.*  
325 *pinaster* showed to be directly dependent on EA pattern variability. For instance, mean  
326 temperature of December and winter of the previous year were highly positively  
327 correlated with EA in December (Fig. 6a) and winter (Fig. 6b), respectively. In addition,  
328 annual temperature was positively correlated with annual EA ( $R = 0.49$ ,  $P = 0.001$ ).  
329 Moreover, water balance in April showed a positive correlation with April EA (Fig. 6c).

330

331

## 332 **Discussion**

### 333 Patterns of IADF occurrence

334 The frequencies of IADFs previously described for different pine species under a wide  
335 variety of climatic conditions were considerably lower than those reported in this paper.  
336 Under boreal or temperate climate, IADFs were observed in 9% of the tree rings at  
337 maximum (Wimmer et al. 2000; Rigling et al. 2001; Copenheaver et al. 2006), and  
338 under Mediterranean climate, they were observed in up to 15–32% of the rings  
339 (Campelo et al. 2006; Bogino and Bravo 2009; Vieira et al. 2009). In our study, eight  
340 out of ten stands showed IADFs in more than 30% of the rings, six stands in more than  
341 50%, and a maximum frequency of 89.5% of the rings with IADFs was found. Despite

342 IADFs are assumed to be special features or anomalies in normal tree-ring growth, in  
343 the light of the observed frequencies, IADFs are more the rule than the exception in *P.*  
344 *pinaster* under mild Atlantic climate.

345         Studies on several pines, including *P. pinaster*, showed that the frequency of  
346 IADFs was negatively related to tree age and positively to growth rates, being more  
347 abundant in the juvenile period and during or immediately after periods with wider rings  
348 (e.g., Copenheaver et al. 2006; Bogino and Bravo 2009; Hoffer and Tardif 2009; Vieira  
349 et al. 2009). Our findings, however, showed no dependence among IADFs frequency,  
350 cambial age, and ring width, which can be due to the reduced age of our trees in  
351 comparison with other works describing age-related effects. However, age-related  
352 effects can be important in determining the high frequency of IADFs observed, since the  
353 sampled trees are not much older than 55 years, and IADFs frequency is usually much  
354 higher for younger trees (Viera et al. 2009).

355         The frequency of IADFs was strongly dependent on elevation, with more  
356 abundant IADFs at lower than higher elevations. These evidences suggest that the  
357 stressful effects of specific triggering factors causing short-term reduction/reactivation  
358 of cambial activity and cell enlargement decrease with increasing elevation. A longer  
359 span of the growing season at a lower elevation has probably also contributed to higher  
360 frequencies of IADFs.

361         As previous publications on pine species (Rigling et al. 2001, 2002; Campelo et al.  
362 2006; Vieira et al. 2009), we found a higher frequency of IADFs in the latewood than in  
363 the earlywood of *P. pinaster*. Reductions of cambial activity at the early growing season  
364 are less likely than a later growth reactivation, probably due to the different duration of  
365 growth periods for early- and latewood, and to more regular weather conditions during  
366 early in the active season. In *P. halepensis* under warmer and xeric conditions,

367 earlywood formation lasts for only two months (March to April-May), while latewood  
368 growth is more time-consuming, extending up to six-eight months from May-June to  
369 November-December (De Luis et al. 2007; Camarero et al. 2010). Accordingly, our  
370 results suggest that latewood growth of *P. pinaster* in NW Spain could last for at least  
371 six months, from May to October-November.

372

### 373 Climatic determinants of wood density fluctuations

374 We interpret the dependency of IADFs on climate on the basis of particular  
375 preconditioning and triggering climatic factors, whose combined effects produced the  
376 observed fluctuations in wood density.

377 Climatic drivers for the occurrence of IADFs in the earlywood of *P. pinaster*  
378 showed to be relatively heterogeneous throughout the study area, with very few IADFs  
379 per stand, while a clear combination of climatic drivers for their formation was  
380 identified at a regional scale. Below-average water availability in previous late summer  
381 (August), or below-average temperature in previous winter (December), are  
382 preconditioning factors for the formation of bands of latewood-like tracheids within the  
383 earlywood. Both factors are related to the amount of carbohydrates stored in the  
384 previous season and used for growth in spring (Hansen and Beck 1994; Lacoïnte 2000).  
385 Water availability in summer can modulate the amount of carbohydrates at the end of  
386 the growing season, considering that summer drought is not as restrictive as under  
387 Mediterranean climate, while photosynthetic activity of *P. pinaster* can be inhibited by  
388 low temperatures during winter (Medlyn et al. 2002). Below-average water balance in  
389 April appears to be the actual triggering factor for IADFs type E, in combination to low  
390 carbohydrate reserves at the beginning of the active season. Such relationships to water  
391 availability in the early growing season were found for other conifers in different



392 regions. For instance, the frequency of IADFs in the earlywood of *P. nigra* in the  
393 northern Alps was negatively correlated with May precipitation (Wimmer et al. 2000),  
394 earlywood density of *Picea abies* in France responded strongly to fluctuations in soil  
395 water reserves in late spring-early summer (Bouriaud et al. 2005), and drought in early  
396 summer induced the formation of IADFs in the earlywood of the Mediterranean pines  
397 *P. pinea* and *P. halepensis* (Campelo et al. 2006; De Luis et al. 2007). Moreover, carbon  
398 gain in winter can be allocated to growth of fine roots, increasing their absorptive  
399 capacity at the onset of following growing season (Lacointe 2000), which can contribute  
400 to proper cell enlargement during the earlywood formation, and thus reduce the  
401 frequency of IADFs type E. These findings highlight the importance of water deficit for  
402 the short-term inhibition of cell enlargement at the beginning of the growing period,  
403 which combined with a low carbon availability can induce false-rings formation in the  
404 earlywood of *P. pinaster* under Atlantic climate.

405       The formation of IADFs type L are triggered by climatic conditions in late spring  
406 and summer, but winter temperature regulating photosynthesis and the amount of  
407 carbohydrates available for the following season seemed to be also a major  
408 preconditioning. Radial growth depends on tree water status as a controlling factor for  
409 the metabolism of the entire tree, but it also depends on the carbon balance as a source  
410 of energy for metabolic activity and of compounds for the cambial activity (Zweifel et  
411 al. 2006). In evergreen conifers, the carbon supply for needle formation and cambial  
412 activity is provided by mobilization of stored reserves, complemented with new  
413 photosynthates assimilated even during the cold season (Hansen and Beck 1994).  
414 Relatively high rates of winter photosynthesis are stimulated by elevated temperatures  
415 in the previous winter (Schaberg et al. 1998; Medlyn et al. 2002), and bands of  
416 earlywood-like tracheids in the latewood seemed to occur less frequently when high

417 temperatures occurred in previous winter. Therefore, a negative carry-over effect due to  
418 less stored carbohydrates seems to be detrimental for growth, probably causing an  
419 inhibition of cambial activity and the earlier beginning of latewood formation due to  
420 limited carbon reserves. If latewood is formed earlier, the probability of cambium  
421 reactivation due to the occurrence of any favorable condition increases.

422       The climatic triggers for IADFs type L had a geographically heterogeneous  
423 distribution within the study area, with two different groups of stands. In coastal stands,  
424 IADFs type L were favored by low temperatures in May-August, when periods of low  
425 water availability are common, though less pronounced than under a Mediterranean  
426 climate (Martínez Cortizas et al. 1994). The high water use efficiency and growth  
427 potential of *P. pinaster* even under moderate water stress (Correia et al. 2008), can  
428 explain the greater frequency of IADFs type L if low temperatures in late spring and  
429 summer alleviate drought stress and promote cambium reactivation. By contrast, a low  
430 water availability coupled with high temperatures in late spring-summer increased the  
431 probability of latewood IADFs occurrence in inland stands. Cambium reactivation may  
432 be promoted by positive water balance at shorter time scales than the monthly periods  
433 adopted in this work, as probably occurs in our inland study stands. These climatic  
434 determinants for IADFs formation are not consistent with those previously described in  
435 the literature, in which the combined effects of cool springs-drought summers (Hoffer  
436 and Tardif 2009), or the succession of cool and warm conditions in the active period  
437 (Rigling et al. 2002) facilitate the formation of IADFs. But these previous works were  
438 performed in boreal pines under other limiting climatic conditions, and they did not  
439 distinguish different types of IADFs according to their intra-ring position, then these  
440 previous studies could not be comparable with our results.

441 Density fluctuations of type L+ were preconditioned by warm/dry conditions  
442 during most of the growing season, particularly by a warm period from March to May  
443 in dry years, and triggered by a wet October. This dependency on climatic factors is  
444 consistent with those described for other Mediterranean pines. In *P. pinea* and *P.*  
445 *halepensis*, the occurrence of a spring-summer drought combined with early autumn  
446 precipitation favored the formation of IADFs in the latewood (Campelo et al. 2006; De  
447 Luis et al. 2007). Moreover, Vieira et al. (2009) showed that IADFs in the late latewood  
448 of *P. pinaster* under Mediterranean conditions are strongly linked to wet autumns,  
449 mainly in October. This response was uniformly observed throughout our study area,  
450 suggesting that the formation of IADFs type L+ responds to very specific climatic  
451 factors, and has a wide geographical and even inter-specific validity among  
452 Mediterranean pine species.

453 A relevant finding of this paper is that IADFs in the earlywood and the early  
454 latewood of *P. pinaster* in NW Spain were strongly linked to the EA pattern, but not  
455 those in the late latewood. This significant connection with EA was due to a direct link  
456 between EA variation and the regional climatic drivers for the formation of IADFs at  
457 the beginning and the middle of the growing season. In particular, regional climate is  
458 strongly related to EA pattern for temperature in previous winter, and also for water  
459 balance in April, which are major preconditioning and triggering factors, respectively,  
460 for the formation of IADFs types E and L. Although some connection between tree-ring  
461 growth and other large-scale patterns, like the North Atlantic Oscillation, have been  
462 previously observed in southern Europe (Piovesan and Schirone 2000; Rozas et al.  
463 2009), this work demonstrates for the first time a strong link between IADFs formation  
464 and the EA pattern, mediated by a robust large-scale modulation of regional climate.

465

466 IADFs and growth plasticity in *P. pinaster*

467 As other Mediterranean pines, *P. pinaster* evolved during the Pliocene under  
468 tropical-like climate, before the onset of the Mediterranean climate, as a component of  
469 the pre-Mediterranean Arcto-Tertiary flora (Verdú et al. 2003; Petit et al. 2005). This  
470 species survived to a past gradual increase of aridity during the transition to  
471 Mediterranean conditions, which may have led to its characteristic growth plasticity  
472 (Chambel et al. 2007). The expected growth behavior should be partially related to the  
473 intra-annual reduction/reactivation of photosynthetic and cambial activities typical of  
474 Mediterranean and subtropical environments showing seasonal aridity (Cherubini et al.,  
475 2003). Also the vegetative cycle of Mediterranean pines is usually markedly bicyclic or  
476 polycyclic, often showing two or more growth units in each annual shoot (Heuret et al.  
477 2006; Barthélémy and Caraglio 2007). Polycyclism is a characteristic expressing  
478 adaptation to intermittent favorable conditions for vegetative growth that is more  
479 frequently expressed under Atlantic humid conditions (Alía et al. 1997). The hormone  
480 indol-3-acetic acid is produced in the younger shoots and exported basipetally to induce  
481 the production of xylem and regulate the developmental processes during xylogenesis  
482 (Aloni 2001), so that we can hypothesize that shoot growth and cambial activity should  
483 be related. Further investigations on intra-annual tree-ring growth based on high-  
484 resolution dendrometer measurements and xylogenesis (e.g., De Luis et al. 2007;  
485 Camarero et al. 2010), and their relationships with shoot enlargement, should inform us  
486 about the physiological and ecological significance of IADFs as adaptive traits.

487

488

489 **Acknowledgements** We thank N. Bermejo, A. González, S. Lamas, P. Manso, B.  
490 Rodríguez-Morales and A. Soliño for field and laboratory assistance. The personnel

491 from Dirección Xeral de Montes, Xunta de Galicia, Forest Districts and Islas Atlánticas  
492 National Park facilitated site accession. V. Rozas benefited from research contracts by  
493 INIA-Xunta de Galicia and CSIC. This research was funded by Dirección Xeral de  
494 Investigación, Desenvolvemento e Innovación, Xunta de Galicia  
495 (PGIDIT06PXIB502262PR).

496

497

#### 498 **References**

- 499 Alía R, Moro J, Denis JB (1997) Performance of *Pinus pinaster* provenances in Spain:  
500 interpretation of the genotype by environment interaction. *Can J For Res* 27: 1548–  
501 1559
- 502 Aloni R (2001) Foliar and axial aspects of vascular differentiation: hypotheses and  
503 evidence. *J Plant Growth Regul* 20: 22–34
- 504 Barnston AG, Livezey RE (1987) Classification, seasonality and persistence of low-  
505 frequency atmospheric circulation patterns. *Mon Wea Rev* 115: 1083–1126
- 506 Barthélémy D, Caraglio Y (2007) Plant architecture: a dynamic, multilevel and  
507 comprehensive approach to plant form, structure and ontogeny. *Ann Bot* 99: 375–  
508 407
- 509 Bogino S, Bravo F (2009) Climate and intraannual density fluctuations in *Pinus*  
510 *pinaster* subsp. *mesogeensis* in Spanish woodlands. *Can J For Res* 39: 1557–1565
- 511 Bouriaud O, Leban J-M, Bert D, Deleuze C (2005) Intra-annual variations in climate  
512 influence growth and wood density of Norway spruce. *Tree Physiol* 25: 651–660
- 513 Bucci G, González-Martínez SC, Le Provost G, Plomion C, Ribeiro MM, Sebastiani F,  
514 Alía R, Vendramin GG (2007) Range-wide phylogeography and gene zones in

515 *Pinus pinaster* Ait. revealed by chloroplast microsatellite markers. Mol Ecol 16:  
516 2137–2153

517 Camarero JJ, Olano JM, Parras A (2010) Plastic bimodal xylogenesis in conifers from  
518 continental Mediterranean climates. New Phytol 185: 471–480

519 Campelo F, Nabais C, Freitas H, Gutiérrez E (2006) Climatic significance of tree-ring  
520 width and intra-annual density fluctuations in *Pinus pinea* from a dry Mediterranean  
521 area in Portugal. Ann For Sci 64: 229–238

522 Chambel MR, Climent J, Alía R (2007) Divergence among species and populations of  
523 Mediterranean pines in biomass allocation of seedlings grown under two watering  
524 regimes. Ann For Sci 64: 87–97

525 Cherubini P, Gartner BL, Tognetti R, Bräker OU, Schoch W, Innes JL (2003)  
526 Identification, measurement and interpretation of tree rings in woody species from  
527 Mediterranean climates. Biol Rev 78: 119–148

528 Copenheaver CA, Pokorski EA, Currie JE, Abrams MD (2006) Causation of false ring  
529 formation in *Pinus banksiana*: A comparison of age, canopy class, climate and  
530 growth rate. For Ecol Manage 236: 348–355

531 Correia I, Almeida MH, Aguiar A, Alía R, Soares T, Santos J (2008) Variations in  
532 growth, survival and carbon isotope composition ( $\delta^{13}C$ ) among *Pinus pinaster*  
533 populations of different geographic origins. Tree Physiol 28: 1545–1552

534 De Luis M, Gričar J, Čufar K, Raventós J (2007) Seasonal dynamics of wood formation  
535 in *Pinus halepensis* from dry and semi-arid ecosystems in Spain. IAWA Journal 28:  
536 389–404

537 De Micco V, Saurer M, Aronne G, Tognetti R, Cherubini P (2007) Variations of wood  
538 anatomy and  $\delta^{13}C$  within-tree rings of coastal *Pinus pinaster* showing intra-annual  
539 density fluctuations. IAWA Journal 28: 61–74

- 540 Edmondson JR (2010) The meteorological significance of false rings in eastern redcedar  
541 (*Juniperus virginiana* L.) from the southern great plains, U.S.A. *Tree-Ring Res* 66:  
542 19–33
- 543 Fritts HC (2001) *Tree rings and climate*. Second edition. Blackburn Press, Caldwell
- 544 Girardin M-P, Tardif J, Bergeron Y (2001) Radial growth analysis of *Larix laricina*  
545 from the Lake Duparquet area, Quèbec, in relation to climate and larch sawfly  
546 outbreaks. *Écoscience* 8: 127–138
- 547 Grissino-Mayer HD (2001) Evaluating crossdating accuracy: A manual and tutorial for  
548 the computer program COFECHA. *Tree-Ring Res* 57: 205–221
- 549 Hansen J, Beck E (1994) Seasonal changes in the utilization and turnover of  
550 assimilation products in 8-year-old Scots pine (*Pinus sylvestris* L.) trees. *Trees* 8:  
551 172–182
- 552 Heuret P, Meredieu C, Coudurier T, Coudurier F Barthélémy D (2006) Ontogenetic  
553 trends in the morphological features of main stem annual shoots of *Pinus pinaster*  
554 (Pinaceae). *Am J Bot* 93: 1577–1587
- 555 Hoffer M, Tardif JC (2009) False rings in jack pine and black spruce trees from eastern  
556 Manitoba as indicators of dry summers. *Can J For Res* 39: 1722–1736
- 557 Lacointe A (2000) Carbon allocation among tree organs: A review of basic processes  
558 and representation in functional-structural tree models. *Ann For Sci* 57: 521–533
- 559 Legendre P, Legendre I (1998) *Numerical Ecology*. 2<sup>nd</sup> English edition. Elsevier,  
560 Amsterdam
- 561 Martínez Cortizas A, Castillo Rodríguez F, Pérez Alberti A (1994) Factores que  
562 influyen en la precipitación y el balance de agua en Galicia. *Boletín de la*  
563 *Asociación de Geógrafos Españoles* 18: 79–96

- 564 Masiokas M, Villalba R (2004) Climatic significance of intra-annual bands in the wood  
565 of *Nothofagus pumilio* in southern Patagonia. *Trees* 18: 696–704
- 566 Medlyn BE, Loustau D, Delzon S (2002) Temperature response of parameters of a  
567 biochemically based model of photosynthesis. I. Seasonal changes in mature  
568 maritime pine (*Pinus pinaster* Ait.). *Plant Cell Environ* 25: 1155–1165
- 569 Park Y-I, Dallaire G, Morin H (2006) A method for multiple intra-ring demarcation of  
570 coniferous trees. *Ann For Sci* 63: 9–14
- 571 Petit RJ, Hampe A, Cheddadi R (2005) Climate change and tree phylogeography in the  
572 Mediterranean. *Taxon* 54: 877–885
- 573 Piovesan G, Schirone B (2000) Winter North Atlantic oscillation effects on the tree  
574 rings of the Italian beech (*Fagus sylvatica* L.). *Int J Biometeorol* 44: 121–127
- 575 Rigling A, Waldner PO, Forster T, Bräker OU, Pouttu A (2001) Ecological  
576 interpretation of tree-ring width and intraannual density fluctuations in *Pinus*  
577 *sylvestris* on dry sites in the central Alps and Siberia. *Can J For Res* 31: 18–31
- 578 Rigling A, Bräker O, Schneiter G, Schweingruber F (2002) Intra-annual tree-ring  
579 parameters indicating differences in drought stress of *Pinus sylvestris* forests within  
580 the Erico-Pinion in the Valais (Switzerland). *Plant Ecol* 163: 105–121
- 581 Rodó X, Baert E, Comin FA (1997) Variations in seasonal rainfall in Southern Europe  
582 during the present century: relationships with the North Atlantic Oscillation and the  
583 El Niño-Southern Oscillation. *Clim Dyn* 13: 275–284
- 584 Rozas V (2003) Tree age estimates in *Fagus sylvatica* and *Quercus robur*: testing  
585 previous and improved methods. *Plant Ecol* 167: 193–212
- 586 Rozas V, Lamas S, García-González I (2009) Differential tree-growth responses to local  
587 and large-scale climatic variation in two *Pinus* and two *Quercus* species in  
588 northwest Spain. *Écoscience* 16: 299–310



- 589 Schaberg PG, Shane JB, Cali PF, Donnelly JR, Strimbeck GR (1998) Photosynthetic  
590 capacity of red spruce during winter. *Tree Physiol* 18: 271–276
- 591 Schweingruber FH, Eckstein D, Serre-Bachet F, Bräker O (1990) Identification,  
592 presentation and interpretation of event years and pointer years in  
593 dendrochronology. *Dendrochronologia* 8: 9–38
- 594 Sokal RR, Rohlf FJ (1995) *Biometry: the principles and practice of statistics in*  
595 *biological research*. Third edition. Freeman & Co., New York
- 596 Thornthwaite DW (1948) An approach toward a rational classification of climate.  
597 *Geographical Review* 38: 55–94
- 598 Trigo RM, Pozo-Vázquez D, Osborn TJ, Castro-Díez Y, Gámiz-Fortis S, Esteban-Parra  
599 MJ (2004) North Atlantic Oscillation influence on precipitation, river flow and  
600 water resources in the Iberian Peninsula. *Int J Climatol* 24: 925–944
- 601 Vaganov EA, Schulze E-D, Skomarkova MV, Knohl A, Brand WA, Roscher C (2009)  
602 Intra-annual variability of anatomical structure and  $\delta^{13}\text{C}$  values within tree rings of  
603 spruce and pine in alpine, temperate and boreal Europe. *Oecologia* 161: 729–745
- 604 Verdú M, Dávila P, García-Fayos P, Flores-Hernández N, Valiente-Banuet A (2003)  
605 “Convergent” traits of Mediterranean woody plants belong to pre-Mediterranean  
606 lineages. *Biol J Linn Soc* 78: 415–427
- 607 Vieira J, Campelo F, Nabais C (2009) Age-dependent responses of tree-ring growth and  
608 intra-annual density fluctuations of *Pinus pinaster* to Mediterranean climate. *Trees*  
609 23: 257–265
- 610 Wimmer R, Strumia G, Holawe F (2000) Use of false rings in Austrian pine to  
611 reconstruct early growing season precipitation. *Can J For Res* 30: 1691–1697

612 Zweifel R, Zimmermann L, Zeugin F, Newbery DM (2006) Intra-annual radial growth  
613 and water relations of trees: implications towards a growth mechanism. *J Exp Bot*  
614 57: 1445–1459  
615  
616  
617  
618

619

620 **Table 1** Site and tree characteristics of the *P. pinaster* stands

Stand name	Code	Latitude (N)	Longitude (W)	Elevation (m)	Number of sampled trees	DBH $\pm$ SD (cm)	Age $\pm$ SD (yr)
Monte Aloia	ALO	42° 05'	8° 41'	530	21	46.2 $\pm$ 9.3	33 $\pm$ 6
A Barrela	BAR	42° 32'	7° 51'	620	24	66.7 $\pm$ 15.4	45 $\pm$ 4
A Capelada	CAP	43° 40'	7° 59'	340	23	45.0 $\pm$ 9.0	42 $\pm$ 3
Illa de Cortegada	COR	42° 37'	8° 47'	20	22	54.4 $\pm$ 9.5	52 $\pm$ 6
Monte Insua	INS	43° 08'	9° 09'	10	15	52.8 $\pm$ 11.8	34 $\pm$ 9
Marco da Curra	MCU	43° 22'	7° 53'	590	20	29.6 $\pm$ 3.7	44 $\pm$ 1
Muros	MUR	42° 48'	9° 04'	155	22	56.6 $\pm$ 5.9	54 $\pm$ 3
Trabada	TRA	43° 25'	7° 13'	640	23	45.7 $\pm$ 6.8	50 $\pm$ 5
Verín	VER	42° 04'	7° 33'	855	23	41.6 $\pm$ 3.5	43 $\pm$ 4
Vigo	VIG	42° 12'	8° 39'	365	19	59.6 $\pm$ 8.3	55 $\pm$ 7

621 *DBH* diameter at 1.30 m above ground

622

623

624

625

626 **Table 2** Descriptive statistics of the IADF distributions. The period includes at least

627 five trees

Code	Period	Cores					Rings				
		N	% IADFs	% E	% L	% L+	N	% IADFs	% E	% L	% L+
ALO	1967-2006	36	100.0	33.3	97.2	100.0	1081	54.0	2.3	26.3	35.8
BAR	1961-2006	50	100.0	14.0	94.0	100.0	1951	69.7	0.7	11.9	61.9
CAP	1966-2006	45	97.8	20.0	97.8	97.8	1693	30.7	0.6	14.7	17.2
COR	1953-2005	34	100.0	88.2	100.0	100.0	1541	89.5	9.0	38.8	66.9
INS	1967-2007	26	100.0	61.5	100.0	92.3	822	45.7	2.8	13.7	34.4
MCU	1961-2006	46	100.0	2.2	97.8	100.0	1914	36.1	0.0	13.6	26.8
MUR	1951-2006	42	100.0	30.9	100.0	95.2	2172	56.2	0.8	15.7	47.5
TRA	1951-2006	48	100.0	16.6	95.8	89.6	2427	15.9	0.4	8.4	7.9
VER	1964-2006	48	95.8	27.1	58.3	87.5	1894	18.3	0.7	3.7	13.9
VIG	1951-2007	33	100.0	63.6	100.0	100.0	1563	53.0	3.0	28.3	31.3

628 *N* total number of cores or rings analyzed, % *IADFs* percentage of cores or rings

629 showing intra-annual density fluctuations, % *E*, % *L* and % *L+* percentage of cores

630 or rings showing density fluctuations of the types *E*, *L* and *L+*, respectively

631

632

633

634

635 **Table 3** Mantel tests for the comparison of inter-site distances and differences between  
 636 site elevations, with the similarities between  $F_{\text{stab}}$  site chronologies and chronology  
 637 statistics for the different types of IADFs (ns: non-significant test)

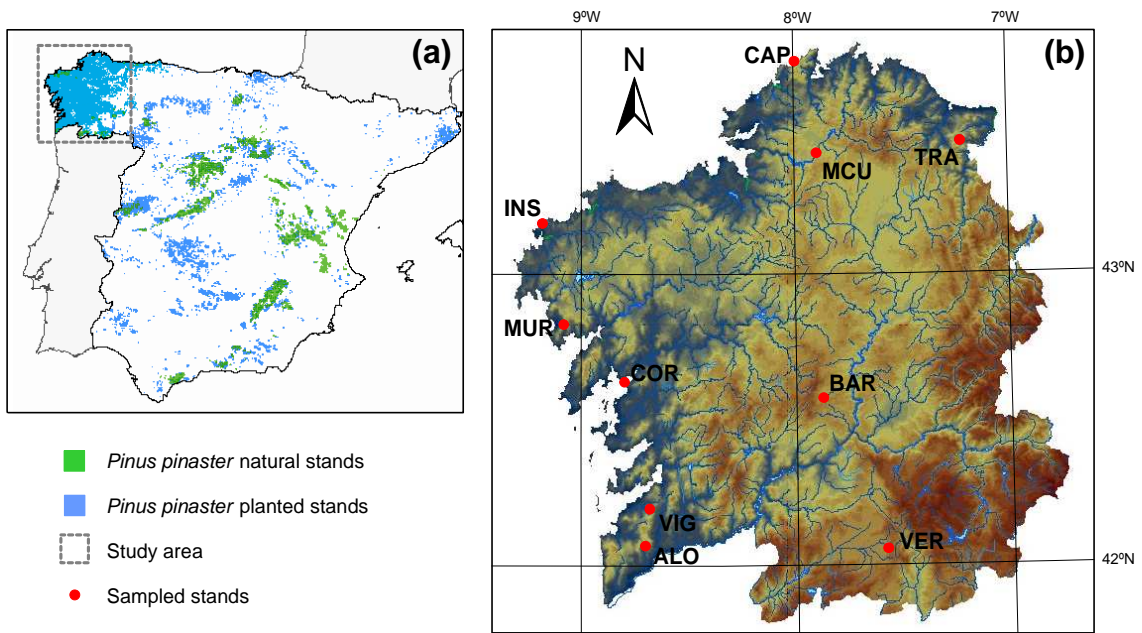
	Variables	Inter-site distances		Site elevations	
		$R_M$	$P$ -value	$R_M$	$P$ -value
IADF chronologies	$F_{\text{stab}}$ E	0.08	ns	0.13	ns
	$F_{\text{stab}}$ L	-0.30	0.021	-0.14	ns
	$F_{\text{stab}}$ L+	-0.15	ns	0.16	ns
IADF chronology statistics	% cores E	0.01	ns	-0.73	<0.001
	% cores L	0.25	ns	-0.64	<0.001
	% cores L+	0.11	ns	-0.24	ns
	% rings IADFs	0.05	ns	-0.57	<0.001
	% rings E	-0.04	ns	-0.61	<0.001
	% rings L	0.07	ns	-0.57	<0.001
	% rings L+	0.04	ns	-0.49	0.001

638

639

640

641



642

643

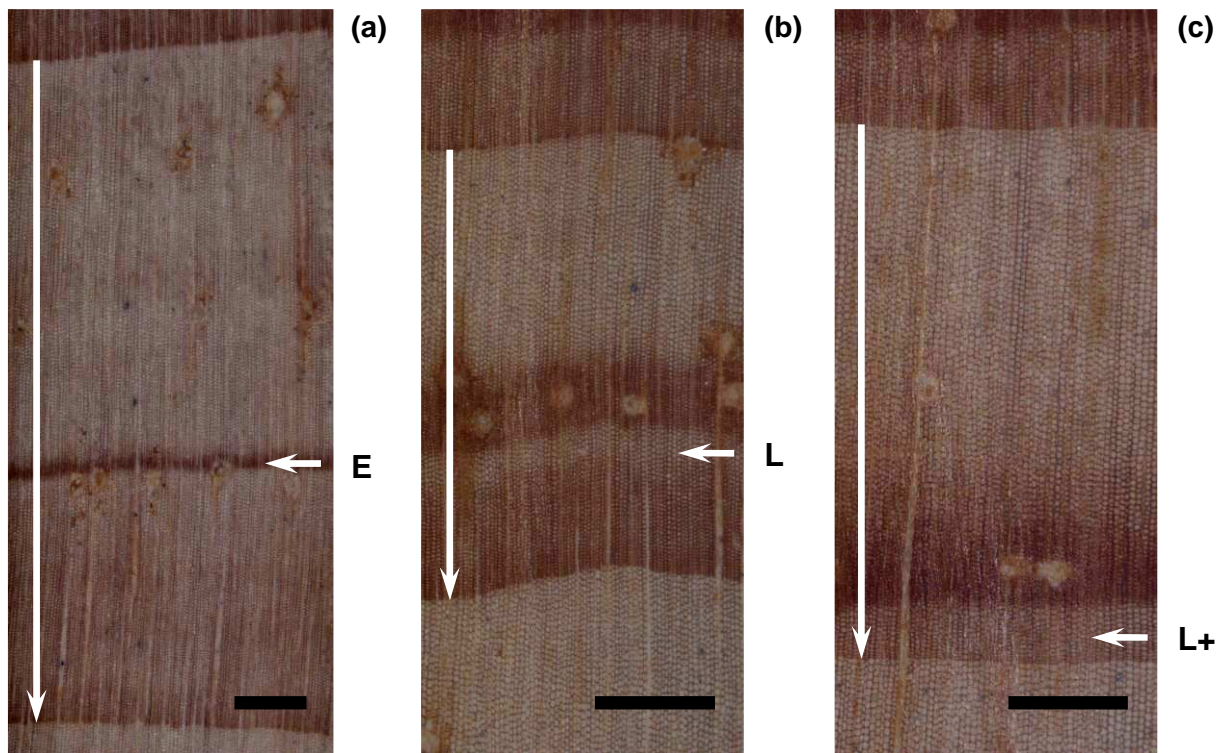
644 **Fig. 1 a** Location of the study area, and distribution of natural and planted *Pinus*  
645 *pinaster* in Spain (<http://iniagis.inia.es/Pinus%20pinaster/>). **b** Location of the sampled  
646 stands in Galicia, NW Spain. Stand codes are shown in Table 1.

647

648

649

650



651

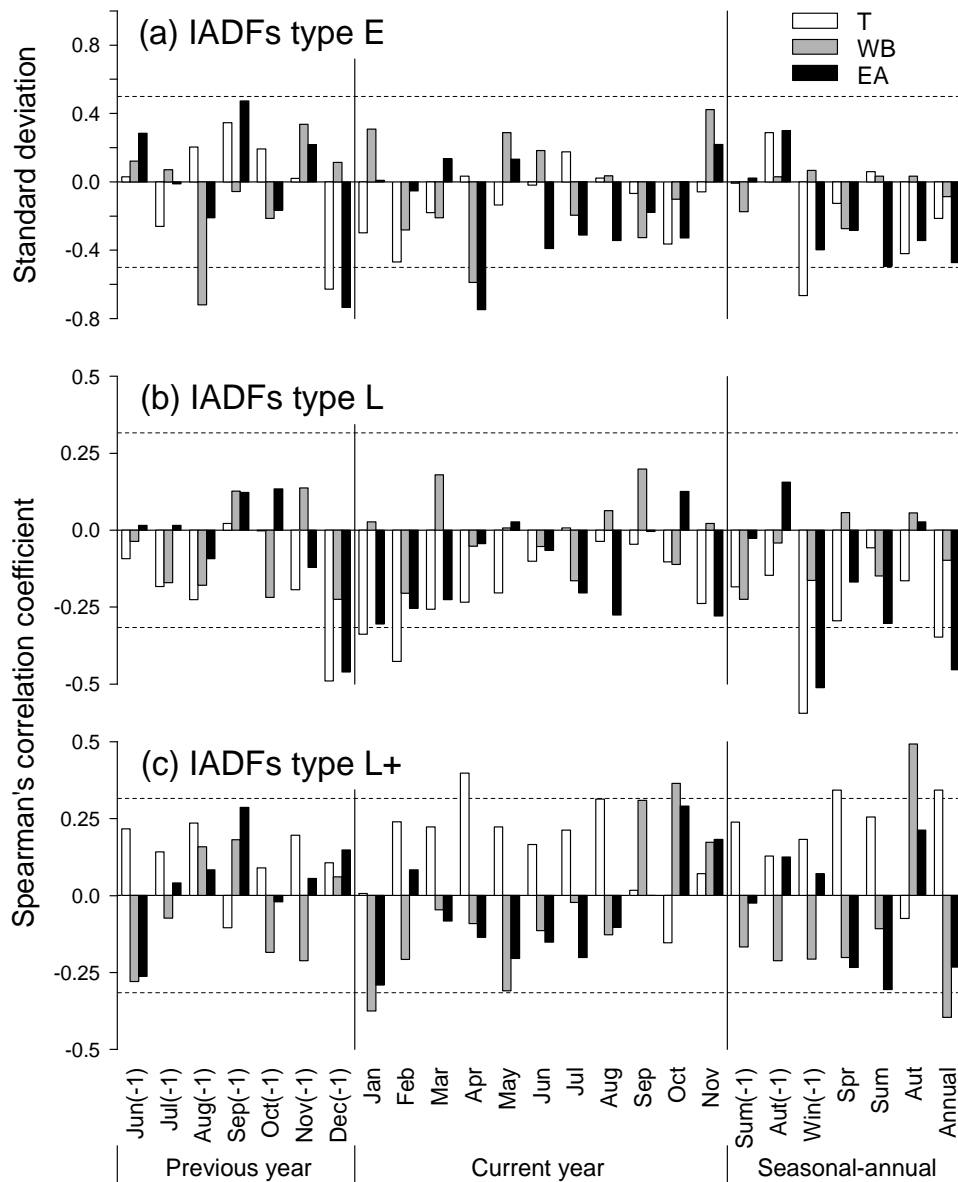
652

653 **Fig. 2** Aspect of the intra-annual wood density fluctuations of the types E **a**, L **b** and L+  
654 **c** in *P. pinaster* based on their anatomical appearance and intra-ring position. Vertical  
655 arrows show the extension of the complete annual ring. E: Latewood-like tracheids  
656 within the earlywood. L: Earlywood-like tracheids within the latewood. L+: Earlywood-  
657 like tracheids near the transition between the latewood and the earlywood of the next  
658 ring. Scale bars: 1 mm

659

660

661

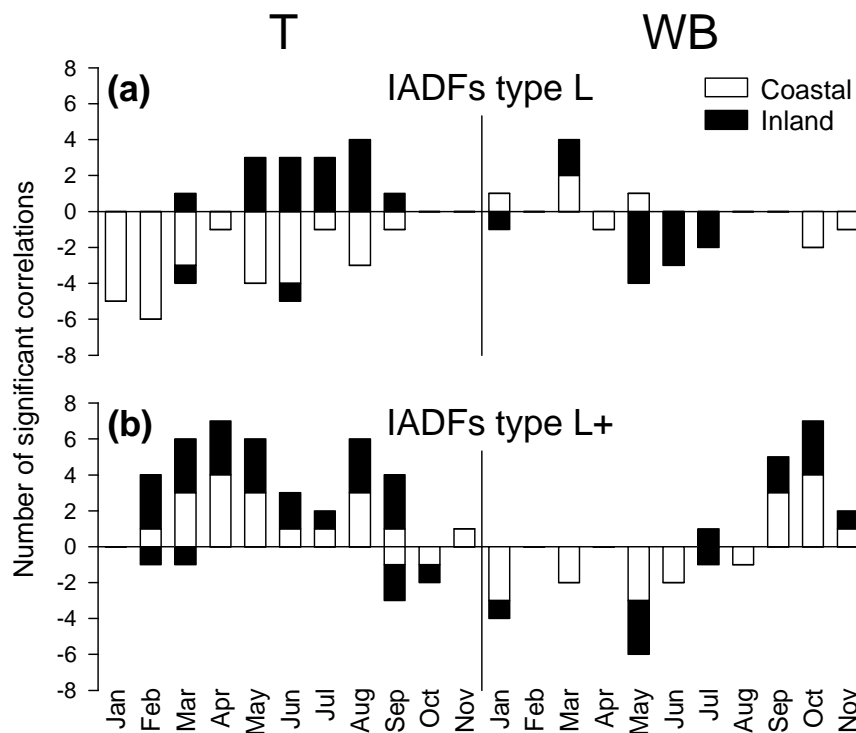


663

664

665 **Fig. 3** Standard deviations from mean temperature (T), water balance (WB) and East  
 666 Atlantic pattern (EA) in those years with significant IADFs type E **a**, and Spearman's  
 667 correlation coefficients between the significant IADFs of types L **b** and L+ **c** and mean  
 668 monthly, seasonal and annual T, WB and EA in the period 1967-2005. Horizontal lines  
 669 indicate the standard deviations  $-0.5$  and  $0.5$ , or the lowest significant ( $P < 0.05$ )  
 670 correlation coefficient, in absolute value





672

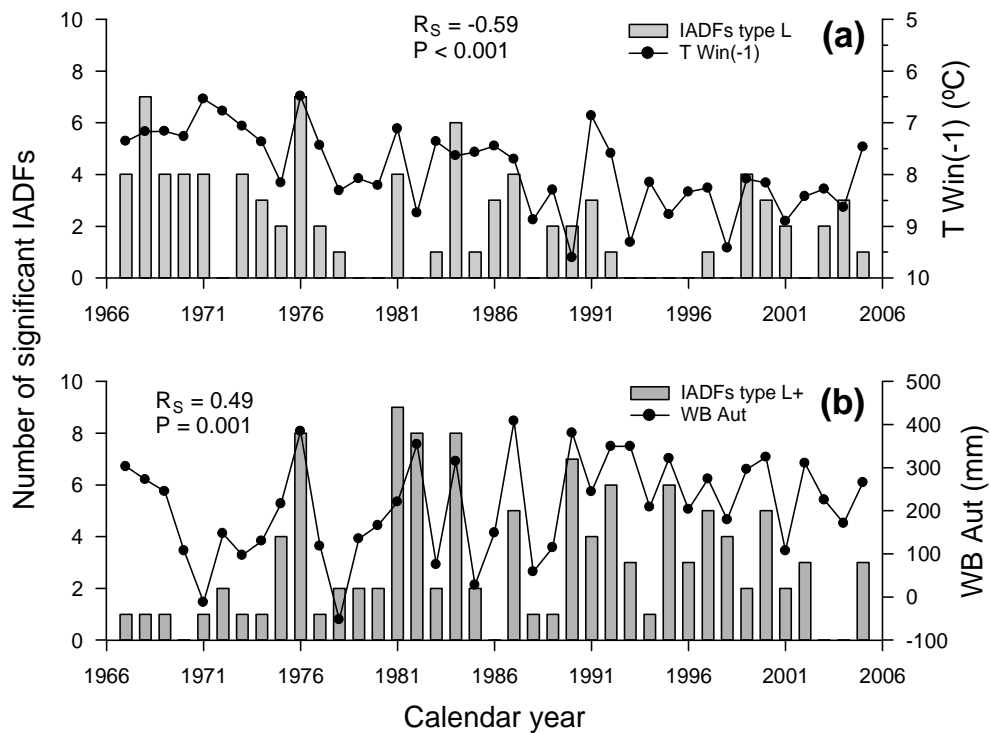
673

674 **Fig. 4** Number of significant Spearman's correlation coefficients between the  $F_{stab}$   
 675 chronologies for IADFs of types L **a** and L+ **b** and local gridded monthly temperature  
 676 (T) and water balance (WB). Coastal (CAP, COR, INS, MUR, VIG) and inland (ALO,  
 677 BAR, MCU, TRA, VER) stands are differentiated. Negative numbers refer to negative  
 678 correlations

679

680

681



683

684

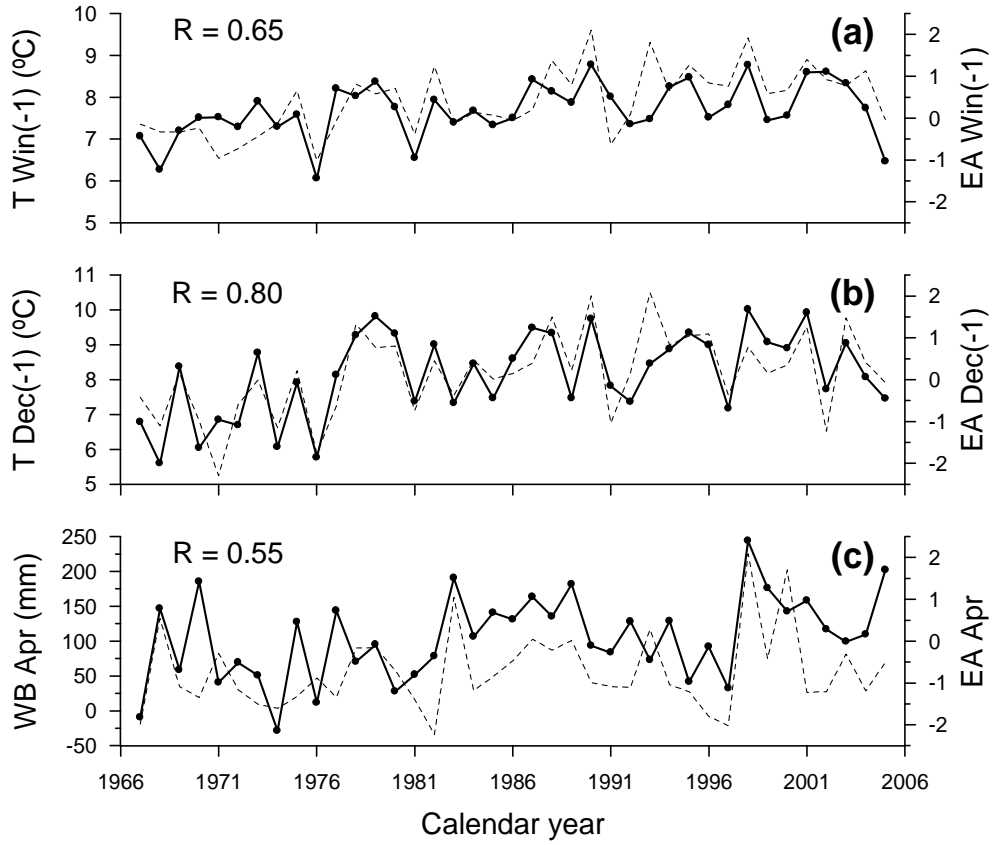
685 **Fig. 5 a** Comparison of the observed number of significant IADFs type L and mean  
 686 temperature (T) in previous winter. Note the reverse scale of T axis. **b** Comparison of  
 687 the observed number of significant IADFs type L+ and water balance (WB) in autumn.  
 688 The Spearman's correlation coefficients ( $R_S$ ) and their significance values ( $P$ ) are  
 689 shown

690

691

692

693



694

695

696 **Fig. 6** Comparison of regional climatic variables for T and WB (dashed lines) and the  
697 EA pattern (solid lines and dots) for previous winter T **a**, previous December T **b**, and  
698 April WB **c**. Pearson's correlations ( $R$ ) between EA and the regional climate series in  
699 1967–2005, all of them significant at the 0.001 level, are shown

700

701